

At the speed of light: Toward a quantum-deterministic description?

Larry M. Silverberg,^{1,a)} Jeffrey W. Eischen,¹ Charles (Chip) B. Whaley, Jr.²

¹*Mechanical and Aerospace Engineering, North Carolina State University, Campus Box 7910, 1840 Entrepreneur Drive, Raleigh, North Carolina 27695-7910, USA*

²*2425 Arbor Hill Road, Canton, Georgia 30115, USA*

(Received 19 April 2024; accepted 16 August 2024; published online 4 September 2024)

Abstract: We examine the quantum-deterministic hypothesis that subatomic bodies consist of an immense number of primitives (particles or fragments of energy) traveling at or near the speed of light. Drawing on the well-proven principle of light and principle of impetus for the deterministic theories, we setup corresponding principles that govern interactions between primitives. Then, we studied the stability of a variety of structures formed from the primitives. One of the primitives for which we present preliminary results has similarities to the photon. These findings suggest a possible relationship between quantum-deterministic and quantum-statistical models and likenesses noticed across realms that we now see as different. © 2024 *Physics Essays Publication*. [<http://dx.doi.org/10.4006/0836-1398-37.4.229>]

Résumé: Nous examinons l'hypothèse déterministe quantique selon laquelle les corps subatomiques sont constitués d'un nombre immense de primitives (particules ou fragments d'énergie) voyageant à la vitesse de la lumière ou à une vitesse proche de celle-ci. En nous appuyant sur le principe de la lumière et le principe d'impulsion, bien établis pour les théories déterministes, nous établissons des principes correspondants qui régissent les interactions entre les primitives. Ensuite, nous avons étudié la stabilité de diverses structures formées à partir des primitives. L'une des primitives, pour laquelle nous présentons des résultats préliminaires, présente des similitudes avec le photon. Ces résultats suggèrent une relation possible entre les modèles quantiques déterministes et quantiques statistiques, ainsi que des similitudes observées entre des domaines que nous considérons maintenant comme différents.

Key words: Deterministic; Gravitation; Light; Photon; Electron; Impetus; Primitive; Quantum; Spacetime; Stability.

I. INTRODUCTION

Quantum mechanics (QM) predicts behavior by the unique quantum-statistical approach of describing electrons as probability clouds (orbitals) that have discrete (quantized) electron energy states.¹ The electrons form into atomic arrangements, and molecular behavior emerges as atoms combine to form molecules through electron sharing (covalent bonds) and transfer (ionic bonds). By this approach, the predictions of molecular structures, energies, and reactions, underpinning modern chemistry and materials science, became very precise—placing QM on a strong foundation. In fact, scientists and science enthusiasts have long regarded the precision attained to be remarkable given that the accomplishment did not require the prediction of the directly unobservable trajectories of subatomic bodies, let alone primitives at some starting scale.

This article examines the prospect of determining the trajectories of primitives toward the development of a quantum-deterministic description. However, unlike past intentions expressed explicitly or implied in the developments of pilot wave theory by de Broglie,² Bohm,³ and others, our intent is not to seek a description that can compete with the quantum-statistical approach in its ability to predict the behavior of molecular structures. Indeed, the

quantum-deterministic description would be much more cumbersome computationally than the quantum-statistical approach. Instead, the underlying intent is to strengthen our understanding of the congruence between QM and the deterministic theories—Newtonian mechanics (NM),⁴ electromagnetism (EM),⁵ special relativity (SR),⁶ and general relativity (GR).⁷ The goal is that of the reductionist—to increase our understanding of the correspondences among the physical theories for the purposes of consolidating terms, terminologies, mathematical techniques, and explanations of the behaviors observed across the physical realms. The quantum-deterministic description might also shed light on assumptions made in the quantum-statistical approach and the standard model. In short, exploring the quantum-deterministic description is an important part of reduction.

In today's deterministic theories, two physical principles stand out—the principle of light and the principle of impetus.⁸ Mathematically, one can formulate both of them as principles of continuity. The transcendence of properties that are mathematical in nature draws one to conject that the principles of light and impetus might apply in some manner to subatomic behavior, too. The focus of this article is on the application of these physical principles to bodies at a primitive scale, toward contributing to the quantum-deterministic description.

NM, EM, and SR describe mathematically the influence that one body has on another by the concept of force. Until recently, the belief was that GR is the exception, that instead

^{a)}lmsilver@ncsu.edu. Tel.: (919) 329 8028.

GR describes influence by a curvature of spacetime. However, recent discoveries have challenged that thinking. It now seems that the concept of force applies to GR, too. For example, in the theory of spacetime impetus (SI),⁸ a new relativistic universal law of gravitation predicts the trajectory of a body when it passes by a gravitational source while traveling at a relativistic speed—in full agreement with the Schwarzschild solution in GR, but without employing the GR apparatus of curved spacetime. It appears that GR hid the concept of force but that it was in there. Furthermore, with the gravitational force's relativistic correction, the universal law of gravitation overcame the inability of SR to account for the influence of a gravitational source. In short, with corrections, one can now describe the influence of a point source by a gravitational force across the deterministic theories of NM, EM, SR, and now GR, too. Note, while inverse square relations hold across the deterministic realms, there are differences between them. They will differ because of the differences in the relativistic linear momentum, which one can reconcile by the Lorentz transformation, and they will differ because of the aggregation that takes place when one moves up in scale (one cannot move down in scale because of irreversibility). Moreover, knowing that the inverse square relations hold across the deterministic theories, there is now more reason to expect the concept of force to apply to subatomic bodies. You will see that the quantum-deterministic approach examined in this article reflects the above-mentioned developments and conjectures.

Section II focuses on the principle of light within the atom. To this end, we draw on observed behavior in free space and hypothesize that the same behavior that applies to free space also applies within the atom, in particular, to bodies at a primitive scale. This becomes the key hypothesis of quantum-deterministic behavior. In support of that hypothesis, Section II deduces the principle of light at an aggregated scale from this hypothesis.

Section III turns to the principle of impetus. Continuing with our hypothesis of primitives that travel at the speed of light, we develop an inverse square relation for these primitives. We develop it by drawing on similarities between our hypothesis and the motion of light in EM, and the before mentioned relativistic universal law of gravitation.

After proposing a principle of light and a principle of impetus for the primitive scale, Section IV lays out a methodical approach for examining the stability of bodies formed from a large number of primitives. The purpose of focusing on a large number of primitives is computational—in future research to help with the study of large-order structures, and seek out and study those that are stable.

In Sections V and VI, we give preliminary results from our search for stable structures formed from primitives. The aspiration was that we might be able to find stable structures that exhibit quantum properties—sort of clouds of primitives akin to the orbitals that one describes in QM quantum-statistically. In the deterministic jargon, the hope was for the clouds of orbiting primitives to exhibit a sort of single-mode behavior that possess a fundamental frequency and a corresponding energy level. In Section V, we present a structure that we found that is unstable. It lacked a key ingredient that

a stable structure would require. Indeed, in Section VI, we present a structure that possess that ingredient. The structure was in the shape of a rotating cosine string. It exhibited the sought after stable behavior. The article ends in Section VII with a summary and conclusions.

II. THE PRIMITIVE ORIGIN OF THE MINKOWSKI SPACETIME METRIC

We begin the examination with a derivation of the Minkowski spacetime metric⁹ by setting up primitives that travel at the speed of light and then aggregating them. One presumes primitives that are directly unobservable while their aggregates are directly observable.

A. Averaging scalars and vectors

Before aggregating primitives, we explain why from a simple mathematical property of averaging, one can anticipate obtaining the Minkowski spacetime metric from primitives. Consider the inequality between positive and negative scalars $(1/n) \sum_{i=1}^n |v_i| \geq |(1/n) \sum_{i=1}^n v_i|$.¹⁰ Imagine that v_i ($i = 1, 2, \dots, n$) are the velocities of bodies in which $v_{av} \triangleq |(1/n) \sum_{i=1}^n v_i|$ is their average, interpreted as the speed of an aggregated body. You might ask what bearing this inequality could have on the limiting speed one finds in the principle of light. To answer this question, consider the vector extension of this inequality $(1/n) \sum_{i=1}^n |\mathbf{v}_i| \geq |(1/n) \sum_{i=1}^n \mathbf{v}_i|$. Imagine now that \mathbf{v}_i ($i = 1, 2, \dots, n$) are velocity vectors of constituent bodies whose speeds are the same, equal to $c = |\mathbf{v}_i|$ ($i = 1, 2, \dots, n$), but whose directions are in general different. The speed of the aggregated body formed from them is $v_{av} \triangleq |(1/n) \sum_{i=1}^n \mathbf{v}_i|$. It follows from this vector inequality that the speed of the aggregated body must be smaller or equal to the speed c of the constituent bodies that formed it. For example, consider constituent bodies whose velocity vectors are the unit vectors $\left\{ \begin{pmatrix} \cos \theta_i \\ \sin \theta_i \end{pmatrix} \right\}_{i=1}^n$. The unit magnitudes can correspond to the speed of light in light units ($c = 1$), and the constituent bodies travel in the directions θ_i ($i = 1, 2, \dots, n$). The average speed is

$$v_{av} = \frac{1}{n} \sqrt{n + 2 \sum_{i=1}^{n-1} \sum_{j=i+1}^n \cos(\theta_i - \theta_j)}.$$

When the constituent bodies travel in the same direction ($\theta_i = \theta_j$), their speeds are equal to the average speed of one. Otherwise, the average speed is less than one. We will hereafter refer to constituent bodies that travel at the speed of light as primitives.

B. The hidden primitive origin of time

Time is a count of cycles, yet our subatomic measurement convention for time draws from cycles that are directly unobservable or hidden. Figure 1 shows what a cycle might look like if it were to come from primitives.¹¹ Denote its spatial increment by dL and its corresponding time increment by

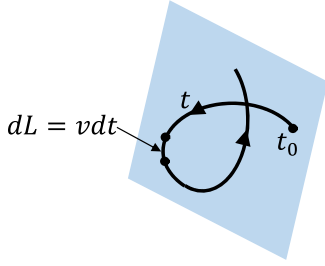


FIG. 1. (Color online) The trajectory of a cycle.

dL . Again, there is no direct measurement of the spatial increment dL or of the time increment dt . Notwithstanding the lack of observability, the length L of the cycle is $\oint dL = cT$ where c is a conversion constant between the chosen unit of length $\oint dL$ and the unit of time T . Let us interpret this conversion constant to be our speed of light. This is tantamount to assuming that primitives travel at the speed of light, mimicking the behavior of light observed in free space.

Returning to the length increment, we can set it equal to $dL = vdt$ and then express the cycle's length as $\oint dL = \oint vdt = cT$, from which $c = (1/T) \oint vdt$ is the average speed over the cycle. Reflecting the mentioned lack of observability, we could let $dL = v_1 dt_1$ or $dL = v_2 dt_2$ without changing dL . However, for simplicity, we can just set v equal to c , that is, assume that the speed of the time increment is constant through the cycle, although it is not strictly necessary to do so.

C. The Minkowski spacetime metric

Continuing with our mimicking of behavior observed in free space, let us now consider a set of n trajectories at the primitive scale, in which each primitive travels at the speed c . We write the length increment of any one trajectory as the displacement vector $d\mathbf{r} = dL\mathbf{e}$, where \mathbf{e} denotes a unit vector tangent to the spatial path. Dividing both sides by dt , the velocity vector of the point is $\mathbf{v} = c\mathbf{e}$. Now, to keep track of primitives, we denote the displacement vector increments of the primitives by $d\mathbf{r}_i = dL\mathbf{e}_i$ ($i = 1, 2, \dots, n$). Due to the generality of this setup, the bodies could be primitives of an aggregated body but they do not have to be. If they are primitives of an aggregated body then the implication is that the primitives formed a structure of some sort. If not, the primitives may be following trajectories out in free space, not belonging to a structure. The primitives can belong to a structure or travel in free space. Right now, our interest is to examine how one moves up in scale from primitives to an aggregated body, so it is best to think of them as belonging to a structure. We define the spatial path increment of a structure to be the average of the spatial path increments of its primitives, written as

$$d\mathbf{r} \triangleq \frac{1}{n} \sum_{i=1}^n d\mathbf{r}_i = \frac{1}{n} \sum_{i=1}^n dL\mathbf{e}_i = \frac{dL}{n} \sum_{i=1}^n \mathbf{e}_i. \quad (1a)$$

Taking the magnitude of both sides, we get $|d\mathbf{r}| = (dL/n) |\sum_{i=1}^n \mathbf{e}_i| \leq (dL/n) \sum_{i=1}^n |\mathbf{e}_i| = dL$. It follows that the magnitude $v_{av} \triangleq |d\mathbf{r}|/dt$ of a structure's velocity vector is less than the speeds $c = dL/dt$ of its primitives unless

all of their motions happen to align (during which $|\sum_{i=1}^n \mathbf{e}_i| = n$).

Next, we seek a relationship between the structure's behavior, which one observes at an aggregated scale, and its unobservable or hidden internal behavior. We find it by defining relative displacement vectors as displacement vectors of primitives relative to the structure's displacement vector $d\mathbf{r}$ as

$$d\mathbf{u}_i \triangleq d\mathbf{r}_i - d\mathbf{r}, \quad (i = 1, 2, \dots, n). \quad (2)$$

Note that we observe the structure's displacement vector $d\mathbf{r}$ at the aggregate scale but not the displacement vectors $d\mathbf{r}_i$ ($i = 1, 2, \dots, n$) of primitives. Next, summing over i , the square of the standard deviation ds of the increments of the relative displacement vectors $d\mathbf{u}_i$ ($i = 1, 2, \dots, n$) is

$$ds^2 \triangleq \frac{1}{n} \sum_{i=1}^n d\mathbf{u}_i \cdot d\mathbf{u}_i. \quad (3a)$$

The standard deviation ds could characterize the structure's internal workings and this might very well serve as a useful property for a structure. From Eq. (2),

$$d\mathbf{u}_i \cdot d\mathbf{u}_i = (d\mathbf{r}_i - d\mathbf{r}) \cdot (d\mathbf{r}_i - d\mathbf{r}) = d\mathbf{r}_i \cdot d\mathbf{r}_i + d\mathbf{r} \cdot d\mathbf{r} - 2d\mathbf{r}_i \cdot d\mathbf{r}.$$

Substituting Eqs. (1a) and (2) into Eq. (3a),

$$\begin{aligned} ds^2 &= \frac{1}{n} \left[\sum_{i=1}^n d\mathbf{r}_i \cdot d\mathbf{r}_i + d\mathbf{r} \cdot d\mathbf{r} \left(\sum_{i=1}^n 1 \right) - 2 \left(\sum_{i=1}^n d\mathbf{r}_i \right) \cdot d\mathbf{r} \right] \\ &= \frac{dL^2}{n} \sum_{i=1}^n \mathbf{e}_i \cdot \mathbf{e}_i + d\mathbf{r} \cdot d\mathbf{r} - 2d\mathbf{r} \cdot d\mathbf{r} \\ &= c^2 dt^2 - d\mathbf{r} \cdot d\mathbf{r}. \end{aligned}$$

Thus,

$$ds^2 = c^2 dt^2 - d\mathbf{r} \cdot d\mathbf{r}, \quad d\mathbf{r} \cdot d\mathbf{r} = d\mathbf{r} \cdot d\mathbf{r}. \quad (4)$$

Equation (4) is precisely the Minkowski spacetime metric at the aggregated scale.

Remark: The derivation given above defined the position vector \mathbf{r} and the velocity vector \mathbf{v} of a structure as an average of primitive position vectors and primitive velocity vectors, respectively, and it invoked a standard deviation ds . However, we could have started differently, by taking weighted averages and by invoking a weighted standard deviation. The weighted averages of position vectors and velocity vectors are a position vector and a velocity vector of the system's mass center. In terms of the weighted quantities, instead of Eqs. (1a) and (3a), we could have started with

$$d\mathbf{r} \triangleq \frac{1}{m} \sum_{i=1}^n m_i d\mathbf{r}_i, \quad m = \sum_{i=1}^n m_i, \quad (1b)$$

$$ds^2 \triangleq \frac{1}{m} \sum_{i=1}^n m_i d\mathbf{u}_i \cdot d\mathbf{u}_i. \quad (3b)$$

Replacing standard quantities with weighted quantities does not change the outcome of the subsequent steps. We would

have still obtained the Minkowski spacetime metric. However, this occurred only because we had started with subatomic bodies traveling at the speed c .

D. Physical interpretation of the spacetime metric

The derivation given above provides us with a plausible physical interpretation of the spacetime metric. In spacetime physics, we ordinarily think of the spacetime increment ds at an observed scale, as an increment along a line,¹² and do not associate it with a composition or with constituent elements that correspond to a smaller scale. The increment itself is an aggregate but we disregard this fact in the mathematical description, even though no one has ever measured anything that is devoid of a composition. With this derivation of the Minkowski spacetime metric, we now can interpret the measurement as coming from an aggregate. In particular, we can interpret the spacetime increment ds as the standard deviation over a time increment of relative displacement vectors of primitives composing a subatomic structure.

We see that the setup at a primitive scale led to the Minkowski spacetime metric, from which one deduces that the speed of light is the same in any frame of reference. Juxtapose that with primitives traveling at the speed c in a spatial framework that comes prior to the construction of a Minkowski spacetime metric. The primitives by themselves would not satisfy the spacetime metric. Therefore, if we were to consider individual primitives in another frame of reference, the speed of each primitive would no longer have been c . Thus, the setup demands the existence of a single frame—the starting assumption of a universal frame. Only then, would the setup not suffer from contradictions. This realization aligns closely with the Newtonian concept of the inertial frame and with Foucault and Mach’s universal frame in Newtonian space, and with Einstein’s support of the universal frame in spacetime.

For further clarity about the meaning of spacetime, imagine a body composed of just two primitives, recognizing that the number of primitives would be immense, not just two. Recall that we do not observe them directly but assume that this is where our measurements come from. The two primitives are rotating about the z -axis while traveling upward in the z direction, too (see Fig. 2). As shown, their position vectors and velocity vectors at the instant shown are $\mathbf{x}_1 = R\mathbf{i}$, $\mathbf{v}_1 = R\omega\mathbf{j} + V\mathbf{k}$, $\mathbf{x}_2 = -R\mathbf{i}$, and $\mathbf{v}_2 = -R\omega\mathbf{j} + V\mathbf{k}$. The radius is R , the angular rate is ω , and the component of velocity in the z direction is V . Finally, as required, the speed

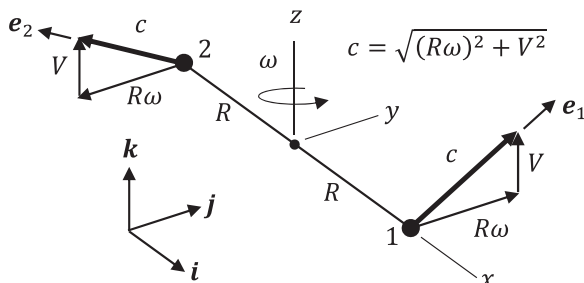


FIG. 2. Example.

of each primitive is equal to the speed of light $c = \sqrt{(R\omega)^2 + V^2}$.

The observation focuses on the system as a whole, the average location of the system and its rate of change over time. Over a time increment dt , the two primitives undergo the displacement vector increments $d\mathbf{x}_1 = \mathbf{v}_1 dt = (R\omega\mathbf{j} + V\mathbf{k})dt = cdt\mathbf{e}_1$ and $d\mathbf{x}_2 = \mathbf{v}_2 dt = (-R\omega\mathbf{j} + V\mathbf{k})dt = cdt\mathbf{e}_2$, where $\mathbf{e}_1 = \frac{R\omega}{c}\mathbf{j} + \frac{V}{c}\mathbf{k}$ and $\mathbf{e}_2 = -\frac{R\omega}{c}\mathbf{j} + \frac{V}{c}\mathbf{k}$ are the unit vectors that point in their respective directions. As unit vectors, we know that $\mathbf{e}_1 \cdot \mathbf{e}_1 = \mathbf{e}_2 \cdot \mathbf{e}_2 = 1$. Over the time increment, one finds the average displacement vector of the system as follows:

1. Define the average displacement vector of the two primitives as $d\mathbf{x} \triangleq (1/2)(d\mathbf{x}_1 + d\mathbf{x}_2)$.
2. Substitute $d\mathbf{x}_1$ and $d\mathbf{x}_2$ into the definition $d\mathbf{x}$ and get

$$\begin{aligned} d\mathbf{x} &= \frac{1}{2}cdt(\mathbf{e}_1 + \mathbf{e}_2) = \frac{1}{2}cdt\left(\frac{R\omega}{c}\mathbf{j} + \frac{V}{c}\mathbf{k} - \frac{R\omega}{c}\mathbf{j} + \frac{V}{c}\mathbf{k}\right) \\ &= vdt\mathbf{k}. \end{aligned}$$

The magnitude of $d\mathbf{x}$ is vdt , where the average velocity is $v = V$. The velocity vector $\mathbf{v} = v\mathbf{k}$ acts in the \mathbf{k} direction. Next, we look at the standard deviation of the displacement vectors of the primitives. Over the time increment dt , one finds the standard deviation squared as follows:

1. Define the standard deviation squared as $ds^2 \triangleq (1/2)\{|d\mathbf{x}_1 - d\mathbf{x}|^2 + |d\mathbf{x}_2 - d\mathbf{x}|^2\}$.
2. The magnitude squared of a vector is the dot product of the vector with itself. Substitute $d\mathbf{x}_1$, $d\mathbf{x}_2$ and their average $d\mathbf{x}$ into ds^2 , and get

$$\begin{aligned} ds^2 &= \frac{1}{2}\{(cdt\mathbf{e}_1 - vdt\mathbf{k}) \cdot (cdt\mathbf{e}_1 - vdt\mathbf{k}) \\ &\quad + \{(cdt\mathbf{e}_2 - vdt\mathbf{k}) \cdot (cdt\mathbf{e}_2 - vdt\mathbf{k})\} \\ &= \frac{1}{2}(c^2(dt)^2(\mathbf{e}_1 \cdot \mathbf{e}_1 + \mathbf{e}_2 \cdot \mathbf{e}_2) - vc(dt)^2(\mathbf{e}_1 + \mathbf{e}_2) \cdot \mathbf{k} \\ &\quad + v^2(dt)^2(\mathbf{k} \cdot \mathbf{k})) = c^2(dt)^2 - 2v^2(dt)^2 + v^2(dt)^2 \\ &= (c^2 - v^2)(dt)^2. \end{aligned}$$

The result is $ds = cd\tau = \sqrt{c^2 - v^2}dt$. This equation describes the standard deviation of the system over the time increment. In this example, we considered two primitives but the result will be $ds = cd\tau = \sqrt{c^2 - v^2}dt$ with any number of primitives traveling at the speed of light. Notice, as the average speed v of the primitives gets larger that $\sqrt{c^2 - v^2}$ gets smaller. The difference between the velocity vectors decreases as their rotational components decrease.

We also showed this in a video simulation.^{b)} As shown, two primitives orbit around each other in a horizontal plane while moving upward. The video contains ten examples with increasing external velocities (average velocities upward).

^{b)}See <http://tinyurl.com/TwoPrimitives> for “Two primitives in orbit.”

For each example, the left figures show the top down view, which reveals only the internal components of the velocity vector, the middle figure, which is a three-dimensional view, and the right figure, which shows a triangle. The diagonal side of the triangle is the magnitude c of the velocity vector, its vertical side is the external velocity v acting upward, and the horizontal side is the internal velocity component circling the system's center.

With respect to the essence of our understanding of spacetime over a time increment, the new realization supports the employment of a primitive scale, and with an aggregated scale, where the Minkowski spacetime metric applies. It provides us with a new rationale for why the spacetime metric is independent of the frame of reference. It requires that a structure composed of primitives, which we characterized by the standard deviation ds , serve as a universal reference. One can now imagine a stationary clock that derives its measurements from hidden rhythms, for which $ds^2 = c^2 dt^2 - dl^2 = c^2 dt^2$ ($dl = 0$). We then define $ds = cd\tau$, where we refer to τ as proper time. Thus, $d\tau = dt$ becomes the stationary clock's time measurement. For the moving clock, the dt changes but $d\tau$ remains the same. We can imagine distributing these stationary clocks over space. At a given instant, they have the same $d\tau$ but measure different dt .

Next, moving from an increment of a trajectory, let us revisit how one interprets the spatial and temporal coordinates of the trajectory over time of a body that travels at speeds ranging from 0 to c . The spacetime increment ds of a body is now changing over time. First, let $dl = 0$. When $dl = 0$, the structure is stationary and $ds = cdt$. This is the largest value that ds can assume over a time increment dt . Next, we increase the speed of the structure. We let $dl = vdt$ for some $v < c$; the structure is now traveling at speed v . The spacetime increment $ds = \sqrt{c^2 - v^2}dt$ is smaller than the spacetime metric $ds = cdt$ for the same dt . At the limit, when $dl = cdt$, the structure travels at the speed c , and $ds = 0$. The standard deviation now assumes its smallest value. As we found earlier, when $v = c$, the primitives in the structure are all aligned; the structure has degenerated to primitives traveling through free space. At this extreme, the structure has really fallen apart. Mathematically, there may be a discontinuity in ds at $v = c$, in the neighborhood over which the structure falls apart, ending when $ds = 0$ (see Fig. 3). This suggests that an aggregated body, which are the structures that we observe, can travel at a speed that is very near—the speed of light but not precisely reach the speed of light—that we should take the speed of light to be a limiting speed.

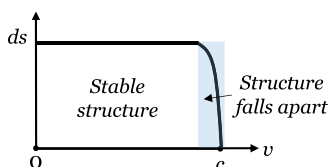


FIG. 3. (Color online) The spacetime metric ds versus speed v .

III. THE PRIMITIVE INVERSE SQUARE LAW

Section II showed that the invariance of the Minkowski spacetime metric at the aggregated scale is rooted in an invariant spatial metric at the primitive scale. Thus, we will employ the spatial metric in our development of an inverse square law for primitives.

No inverse square law presently exists at a primitive scale so, to acquire one, it is perhaps best to draw on what we know about inverse square laws in the deterministic theories. For one, the relativistic universal law of gravitation, although it only applies at the aggregated scale, produces a gravitational force that becomes perpendicular to the direction of motion of a body when its speed approaches that of light. One also recognizes that its form simplifies both when the speed of a body is nonrelativistic but also when the body's speed reaches that of light. In EM, one finds a simplification of this kind in the Biot–Savart inverse square relation for the magnetic force vectors.¹³ This pattern suggests, as one moves down to the primitive scale, that the form of the inverse square law would be simpler than observed at the aggregated scales.

In this section, due to these and other considerations, we examined an inverse square relation for a gravitational force that is of a simple form—while being perpendicular to the primitive's motion. We let \mathbf{r} denote a position vector that extends from the spatial point of a first gravitational source to the spatial point of a second gravitational source. Each of the two source points travels at the speed c , and we denote the velocity vector of the second source point by \mathbf{v} . The vector component of \mathbf{r} that is perpendicular to \mathbf{v} is (see Fig. 4)

$$\mathbf{r}_\perp = \mathbf{r} - \left(\mathbf{r} \cdot \frac{\mathbf{v}}{c} \right) \frac{\mathbf{v}}{c} \tag{5}$$

In Eq. (5), the speed of light is c , and (\mathbf{v}/c) is a unit vector. Therefore, $(\mathbf{r} \cdot (\mathbf{v}/c))(\mathbf{v}/c)$ is the vector component of \mathbf{r} in the direction of \mathbf{v} . We subtract it from \mathbf{r} to produce the vector \mathbf{r}_\perp , which is the component of \mathbf{r} perpendicular to \mathbf{v} .

Having defined \mathbf{r}_\perp , we now define the action force vector acting on the first spatial point of the first source by the second source, located at the second spatial point, as

$$\mathbf{P} = G \frac{m}{r^2} \left(\frac{\mathbf{r}_\perp}{|\mathbf{r}|} \right) \tag{6}$$

Equation (6) is the inverse square law of the gravitational action force vector \mathbf{P} by the second source having mass m

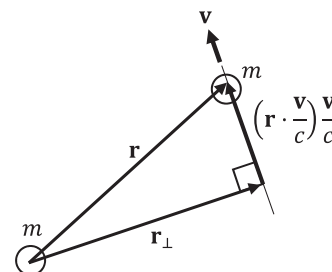


FIG. 4. Vector component \mathbf{r}_\perp perpendicular to the direction of travel.

acting on the first source, also having mass m . The distance between the two sources is $r = |\mathbf{r}|$. By definition, the action force vector is equal to the interaction force vector \mathbf{F} divided by the mass on which it acts ($\mathbf{P} = \mathbf{F}/m$).¹⁴

Remark. Notice above when $\mathbf{r}_\perp = 0$ that $\mathbf{P} = 0$. In the relativistic law of gravitation, which applies to the general relativistic motion of aggregated bodies, one also finds that $\mathbf{P} = 0$ under the same condition $\mathbf{r}_\perp = 0$.¹⁴

Applying Eq. (6) and the principle of impetus to a system of N primitives ($a = 1, 2, \dots, N$), we arrive at the following equations governing the motion of the primitives:

$$\mathbf{P}_{ab} = G_e \frac{m_a}{r_{ab}^2} \left(\frac{\mathbf{r}_{ab\perp}}{|\mathbf{r}_{ab}|} \right), \quad \mathbf{r}_{ab} = \mathbf{r}_b - \mathbf{r}_a, \quad (7)$$

$$\mathbf{r}_{ab\perp} = \mathbf{r}_{ab} - \left(\mathbf{r}_{ab} \cdot \frac{\mathbf{v}_a}{c} \right) \frac{\mathbf{v}_a}{c}, \quad (7)$$

$$\mathbf{P}_a = \mathbf{a}_a, \quad \mathbf{P}_a = \sum_{b \neq a}^N \mathbf{P}_{ab}. \quad (8)$$

Equation (7) defines the action force vectors \mathbf{P}_{ab} between sources a and b and Eq. (8) defines the resultant action force vector \mathbf{P}_a that acts on source a , and by the principle of impetus sets it equal to its acceleration vector \mathbf{a}_a .

Remark: For verification purposes, it is easy to show that \mathbf{P}_a is perpendicular to \mathbf{v}_a , which maintains over time the speed of body a at the light limit c . Of course, this is not coincidental. We initially proposed a gravitational force that is perpendicular to the primitive's motion in order to ensure this.

IV. STABILITY OF PRIMITIVES

Roughly, one defines a system of attracting primitives as stable if the primitives stay close to each other, forming a structure. However, this definition does not distinguish between structures in which adjacent primitives stay adjacent. For example, consider higher scale primitives. They form liquid and solid structures in which the adjacency of the higher scale primitives stays intact as opposed to their gaseous structures in which the adjacency does not stay intact. We shall refer to structures that maintain their adjacencies as locally stable. The observation of subatomic structures suggests at the primitive level that the unobserved primitives maintain their local adjacency. Thus, in QM, we surmise orbitals composed of primitives that exhibit behavior that has similarities to rotating or oscillating swarms of bodies that maintain local stability. Furthermore, the trajectories corresponding to an orbital would configure themselves into a single mode that has an associated frequency and energy level. Furthermore, one would expect the number of primitives that are involved in forming these structures to be immense.

Remark: In nonrelativistic motion at an aggregated scale, vibration (including rotation) of a nondissipative deterministic structure is multimodal,¹⁵ whereas the presence of an orbital in the statistical description of subatomic bodies suggests vibration in a single mode and frequency. One hypothesis is that the mechanism behind reaching the single-mode character of stability, over the multimodal character of stability one finds in nonrelativistic motion, is due to primi-

tives traveling at the speed of light. In fact, in 2020, the third author was performing numerical experiments on structures governed by the same inverse square relations described in Sec. III. Starting with a relatively small number of primitives, which Whaley called ‘‘chips,’’ he explored their behavior by simulating their responses to different initial conditions. Through these investigations, he found initial conditions for which the primitives form into orbital-like structures. In the deterministic language, they looked like stable, single-mode structures.

Section V will describe an orbital-like structure. However, before getting to that, we list just a few among a number of possible strategies that one might employ to find and study orbital-like structures, given the challenge of them being composed of a potentially enormous number of primitives.

- (1) **Visualization:** The configurations of orbital-like structures are initially unknown. A good way to find one is to start with a candidate configuration, examine its response, and then iterate on the configuration to approach an orbital-like structure. Visualization serves as a powerful tool for determining how to change a configuration to enhance its stability. This approach led to the rotating ring and the rotating cosine structures described in Sec. V.
- (2) **Analytical measures:** In addition to visualization, which is a powerful qualitative procedure, one can develop measures that quantify a structure's stability over time. The position of the structure has a mean position and a standard deviation that change over time. Both of these quantities can serve as analytical measures. Other measures can serve to characterize the orbital-like configuration and can focus on the mechanism by which a configuration maintains stability.
- (3) **Stability analyses:** One finds a candidate structure by first prescribing some of its coordinates over time. At this stage, the nonprescribed parameters are still unknown. One has prescribed the coordinates in terms of unknown parameters. For example, one might think that a certain configuration is stable but not know how fast it is rotating. The angular rate would be the unknown parameter. There is no guarantee that the prescribed system, because it is conjecture, will satisfy the governing equations, Eq. (8). Putting that aside, one could still use the error in the governing equations as an analytical measure in order to find the unknown angular velocity. One can find the angular velocity that minimizes the error in the governing equations. It would be the ‘‘best’’ angular velocity. In the following, we use the error in the governing equations as the basis of a methodology that can accommodate candidate structures that consist of a large number of primitives.

A. A constrained stability methodology

We now describe a methodology for determining the stability of a system of a potentially large number of primitives.

We begin by prescribing the motion of a candidate structure. We prescribe the motion of each primitive that composes it. The prescribed motion does not need to satisfy the governing equations of motion, so the simulated response does not necessarily match the response of the candidate structure, nor is the simulated response necessarily stable. However, the response of the candidate structure is supposed to be close to what the analyst thinks is the response of a structure that would satisfy the governing equations of motion.

To develop the methodology, we re-examine Eq. (8). In the candidate structure, one has prescribed its N position vectors and velocity vectors. We denote its prescribed position vectors, velocity vectors, and acceleration vectors, respectively, by $\mathbf{r}_a^p, \mathbf{v}_a^p, \mathbf{a}_a^p$, ($a = 1, 2, \dots, N$). For the stability analysis, we set the structure's initial states of the simulated structure equal to the initial states of the candidate structure, but we relax the prescription of the motion over time of a subset of the primitives. We prescribe the motion of the remaining primitives, regarding them as constraints. Without loss of generality, let us relax the constraints on the motion over time of the first n of its primitives, designating them by $\mathbf{r}_a^f, \mathbf{v}_a^f, \mathbf{a}_a^f$, ($a = 1, 2, \dots, n$) and prescribe over time only the motion of the remaining $N - n$ primitives. The equations that govern the motion of the nonprescribed primitives are then

$$\mathbf{p}_a^{fE} = \mathbf{a}_a^f, \quad (a = 1, 2, \dots, n), \quad (9)$$

in which

$$\mathbf{p}_a^{fE} = \sum_{b \neq a}^n \mathbf{P}_{ab}^{fE} + \sum_{b=n+1}^N \mathbf{P}_{ab}^{pE}. \quad (10)$$

In Eq. (10), \mathbf{P}_{ab}^{fE} is the primitive gravitational force vector between two nonprescribed primitives and \mathbf{P}_{ab}^{pE} is between primitive a , which is nonprescribed, and a prescribed primitive b . Numerical integration of Eq. (9) yields \mathbf{r}_a^f ($a = 1, 2, \dots, n$), which reveals an error that one can describe in terms of a measure like

$$e = \sum_{a=1}^n (\mathbf{r}_a^f - \mathbf{r}_a^p) \cdot (\mathbf{r}_a^f - \mathbf{r}_a^p). \quad (11)$$

The error gives a measure over time of the system's stability.

The constrained stability analysis described above can significantly reduce computer time over an unconstrained analysis when the number n of unconstrained primitives is much smaller than the total number of primitives ($n \ll N$) and when the number N of the elements is extremely large. The integrated number of states reduces from $3N$ to $3n$.

B. The discovery of stable structures

The discovery of stable structures was an evolutionary process that began with examining the behavior of a small number of primitives. We now describe the process followed. (For simplicity, I shall here refer to the x_1, x_2 , and x_3 coordinates as X, Y , and Z coordinates, respectively.) The evolution began by considering one primitive by itself. It traveled in a straight line at the speed c in the Z direction. Next, two primitives were considered. In order to stay close to each other over time, they both needed to travel in the Z

direction or close to the Z direction, at least initially. The two primitives stayed together when they were initially traveling in the Z direction, one behind the other in the Z direction because, in this case, the force between them was zero [see the remark below Eq. (6)]. Furthermore, without a Z offset, the system was unstable. When they were initially moving predominantly in the Z direction, but with an XY offset (in an XY plane) and spiraling about the Z -axis, a self-correction became necessary to maintain stability. At a particular initial XY offset, the two primitives did indeed spiral around each other. A video shows the motion.^{c)} For the given XY offset, the geometric center of the two primitives traveled in the Z direction; it did not have any X or Y components. When slightly increasing or decreasing the XY offset, the circular motion in the XY plane became elliptical and differences in the Z locations of the primitives appeared, with the lead primitive alternating. The effect became more prominent by introducing an initial Z offset. With an initial Z offset, an oscillation of the geometric center of the primitives was more prominent.^{d),e)} One might describe this system as not satisfying the conservation of linear momentum at each instant. However, the system did seem to satisfy the conservation of linear momentum over a time average of the response.

Next, the examination expanded to a string of primitives. The initial placement of the primitives was in the ZX plane with the motion of the primitives predominantly moving in the Z direction whilst rotating about the Z -axis. Depending on the shapes of the strings, primitives at the ends flew off, leaving a smaller number of primitives remaining stable. The groups of primitives that flew off often formed "minicosine" shapes, also rotating about the Z -axis. One obtained a sort of alphabet soup of strings of different lengths, some in the shape of cosine functions rotating about the Z -axis. Therefore, in the next step of the evolutionary process, the initial ZX shapes were just set equal to the shape of a cosine function, rotating about the Z -axis. The resulting structure was stable when the initial rotational rate was within an admissible range, with no primitives flying off. The conclusions from these initial studies was that a string of primitives, spaced one after the other along the Z -axis in the shape of the cosine function, traveling predominantly in that direction, can self-correct and maintain its local stability.^{f)} These preliminary results motivated many questions regarding the nature and scope of stable configurations. Among the questions asked, we wondered whether a string of primitives could be locally stable while maintaining a geometric center that is stationary or traveling at a speed that is much smaller than the speed of light, or whether a line of primitives spiraling in a plane perpendicular to a predominant direction of motion would be stable, too. In the following, we present two structures that we studied in detail.

^{c)}See <http://tinyurl.com/FlatSpiralStructure> for "The rotating structure."

^{d)}See <http://tinyurl.com/SpiralStructure-no-zoom> for "The spiraling structure."

^{e)}See <http://tinyurl.com/SpiralStructure-with-zoom> for "The spiraling structure."

^{f)}See <http://tinyurl.com/CosineStructure> for "The rotating cosine structure."

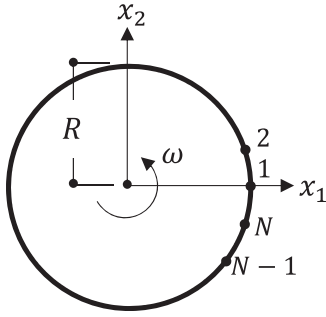


FIG. 5. Idealized rotating ring.

V. THE CIRCULARLY ROTATING RING

The first structure that is interesting to describe in detail is the circularly rotating ring. It consists of N primitives configured in a circle in the $x_1 - x_2$ plane (see Fig. 5). The entire system rotates about the x_3 axis with angular velocity ω , while translating in the x_3 direction with velocity v . The candidate ring consists of $N = 200$ primitives, each a distance R from the x_3 axis. The primitives' locations and velocities are

$$\begin{aligned} x_{a1} &= R \cos(\phi_a), & x_{a2} &= R \sin(\phi_a), & x_{a3} &= vt, \\ v_{a1} &= -\omega R \sin(\phi_a), & v_{a2} &= \omega R \cos(\phi_a), & v_{a3} &= v, \end{aligned} \quad (12)$$

where the polar angles are

$$\phi_a = \frac{a-1}{N-1} 2\pi, \quad (a = 1, 2, \dots, n). \quad (13)$$

In Eq. (12), because the speed of each primitive is c , the velocity v in the x_3 direction is

$$v = \sqrt{c^2 - (\omega R)^2}. \quad (14)$$

The acceleration components of the coordinates are

$$a_{a1} = -\omega^2 R \cos(\phi_a), \quad a_{a2} = -\omega^2 R \sin(\phi_a), \quad a_{a3} = 0. \quad (15)$$

One can calculate easily, because of the symmetries, the angular velocity for which the system satisfies the governing equations. For example, the force components in the x_2 direction on primitive 1 by the other primitives cancel, leaving a sum of force components in the x_1 direction being set equal to a centrifugal effect. One finds that the system's angular velocity is

$$\omega = \left(\frac{GmN}{4R^3} \frac{1}{N} \sum_{a=2}^N \frac{1}{\sin(\phi_a/2)} \right)^{1/2}. \quad (16)$$

Table I gives the simulation data.

Referring to Table I, we selected the values of the constants to be comparable to subatomic scale quantities, but not to correspond to any particular quantities. Notice the one exception is the primitive's mass of 2.567×10^8 kg, which seems inconsistently huge in comparison with the expectedly tiny mass of a primitive. However, we will later find that this uncharacteristically huge value is an artifact of discretiza-

TABLE I. Simulation data for the 200 primitive, rotating ring.

Candidate rotating ring		
m	Primitive mass	2.567×10^8 kg
R	Radius	1.485×10^{-8} m
ω	Angular velocity	9.5×10^{11} rad/s
v_{11}	Initial velocity of primitive 1 in the x_1 direction	0
v_{12}	Initial velocity of primitive 1 in the x_2 direction	-14 100 m/s
v_{13}	Initial velocity of primitive 1 in the x_3 direction	$299\,999\,999.669 \times 10^8$
G	Gravitational constant	6.674×10^{-11} m ³ /kg-s ²
c	Speed of light	3×10^8 m/s

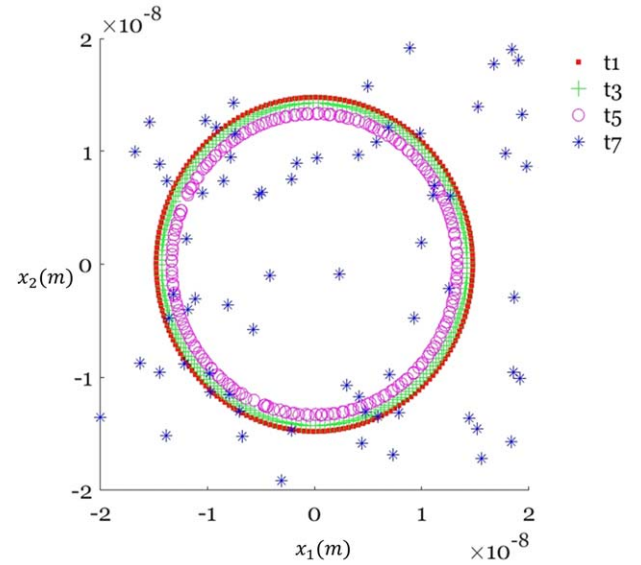


FIG. 6. (Color online) Implosion of the rotating ring's primitives.

tion. We will see later that the actual number of primitives that represents that sought after behaviors would be extremely large in comparison to the 200 primitives considered in the models. Moreover, we will find when increasing the number of primitives that the total mass decreases to a level that one would expect to find at a primitive scale.

Figures 6 and 7 show the short time lapses of primitives 1, 100, and 200 for a time step of $dt = 2.538 \times 10^{-13}$ at $t_1 = dt$, $t_3 = 3dt$, $t_5 = 5dt$, and $t_7 = 7dt$. Two orbits were considered—one for which the angular velocity was set equal to a value that is slightly smaller than the value calculated in Eq. (16) (Fig. 6) and the other for which the angular velocity was slightly larger than the value calculated in Eq. (16) (Fig. 7). For each case, while the 200 primitives followed nearly circular orbits, an instability appeared. The primitives imploded inward for the slightly smaller value of angular velocity (Fig. 6), and the primitives exploded outward for the slightly larger value of angular velocity (Fig. 7).

Thus, as shown, the rotating ring is *not* stable, nor is it even locally stable. The proximate primitives lose their proximity, besides not staying a finite distance from each other. The next example will be both stable and locally stable.

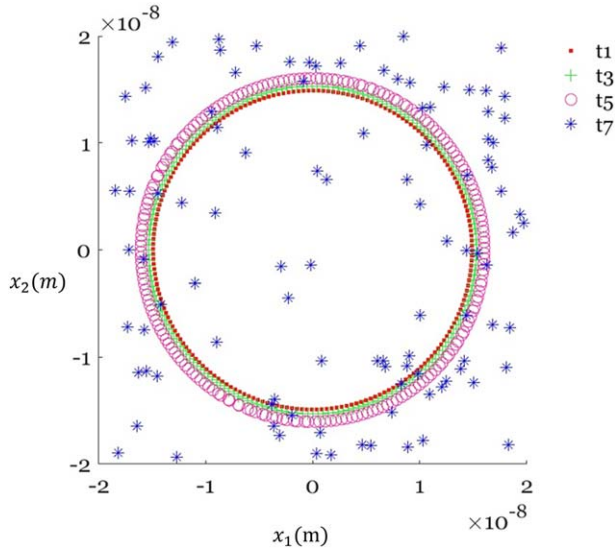


FIG. 7. (Color online) Explosion of the rotating ring's primitives.

VI. THE CIRCULARLY ROTATING COSINE

The circularly rotating cosine structure consists of N primitives in the shape of one wavelength of a cosine function, as shown in Fig. 8. The length L of the idealized circularly rotating cosine is along the x_3 direction such that its primitives are equally spaced along the x_3 direction as they move at a constant speed v in the x_3 direction. The x_3 coordinates of the points at time t are

$$x_{a3} = \frac{a-1}{N-1}L + vt \quad (a = 1, 2, \dots, N). \quad (17)$$

The primitives lie in the $x_3 - r$ plane, where r is the radial length in the $x_1 - x_2$ plane. Its radial coordinates are

$$r_a = R \cos\left(\frac{2\pi x_{a3}}{L}\right), \quad (a = 1, 2, \dots, N). \quad (18)$$

The idealized structure (and the $x_3 - r$ plane) rotates about the x_3 axis at a constant angular velocity ω . Thus, the x_1 and x_2 coordinates of the points at time t , along with their first and second time derivatives, are

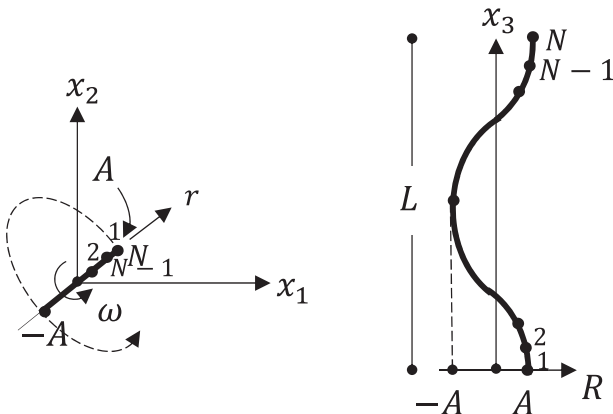


FIG. 8. Idealized rotating cosine structure.

$$\begin{aligned} x_{a1} &= R \cos(\omega t) \cos(2\pi x_{a3}), & x_{a2} &= R \sin(\omega t) \cos(2\pi x_{a3}), \\ v_{a1} &= -\omega R \sin(\omega t) \cos(2\pi x_{a3}), & v_{a2} &= \omega R \cos(\omega t) \cos(2\pi x_{a3}), \\ a_{a1} &= -\omega^2 R \cos(\omega t) \cos(2\pi x_{a3}), & a_{a2} &= -\omega^2 R \sin(\omega t) \cos(2\pi x_{a3}). \end{aligned} \quad (19)$$

In the given examples, the components of the velocity vector in the $x_1 - x_2$ plane are small compared to the speed of light ($\omega R \ll c$), leaving the predominant motion of the primitives to be in the x_3 direction, given that each body is traveling at the speed c . The speeds of the primitives in the x_3 direction are

$$v_a = \sqrt{c^2 - (\omega r_a)^2} \quad (a = 1, 2, \dots, N). \quad (20)$$

Notice, because the radii r_a ($a = 1, 2, \dots, N$) of the primitives differ from one another, the constraint that all the primitives have the same speed results in velocity components v_a ($a = 1, 2, \dots, N$) in the x_3 direction that differ from one another, too. The differences, if constant, would cause the distances between the primitives to grow over time, preventing the idealized shape from being stable. However, we will see that the simulated response, which satisfies the governing equations, will reveal a self-correction that stabilizes the structure.⁵

Table II gives the simulation data. The values of the velocity components of primitive 1 in the x_1 and x_3 directions give the reader an appreciation of the relative differences in their magnitudes. As in the rotating ring problem (Table I), we selected the values of the constants to be comparable to subatomic scale quantities, with the exception of the primitive's mass, for the same reasons given earlier. At the end of this example, we will explain the reason for the seemingly inconsistent value of mass.

We integrated the equations of motion using the fourth-order Runge-Kutta method over a time interval of $0 \leq t \leq 1.1735 \times 10^{-10}$ s. Figures 9 and 10 show the orbits of primitives 1, 100, and 200. The orbits are essentially circular for the parameters used in the simulation. As shown, the rotating cosine is both stable and locally stable.

We will now address the question raised earlier about the uncharacteristically large value of mass that we selected

TABLE II. Simulation data for the 200 primitive, rotating cosine.

Candidate rotating cosine		
m	Primitive mass	2.567×10^8 kg
L	Length	500×10^{-9} m
R	Amplitude	1.485×10^{-8} m
ω	Angular velocity	-6.735×10^{10} rad/s
v_{11}	Initial velocity of primitive 1 in x_1 direction	0
v_{12}	Initial velocity of primitive 1 in x_2 direction	-1000 m/s
v_{13}	Initial velocity of primitive 1 in x_3 direction	$2.999\,999\,999\,98 \times 10^8$
G	Gravitational constant	6.674×10^{-11} m ³ /kg-s ²
c	Speed of light	3×10^8 m/s

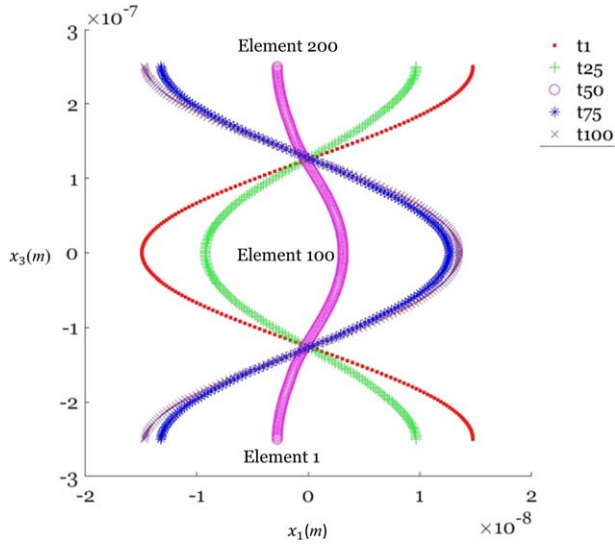


FIG. 9. (Color online) Orbits of primitives 1, 100, and 200 of the rotating cosine (relative to the primitives' geometric center).

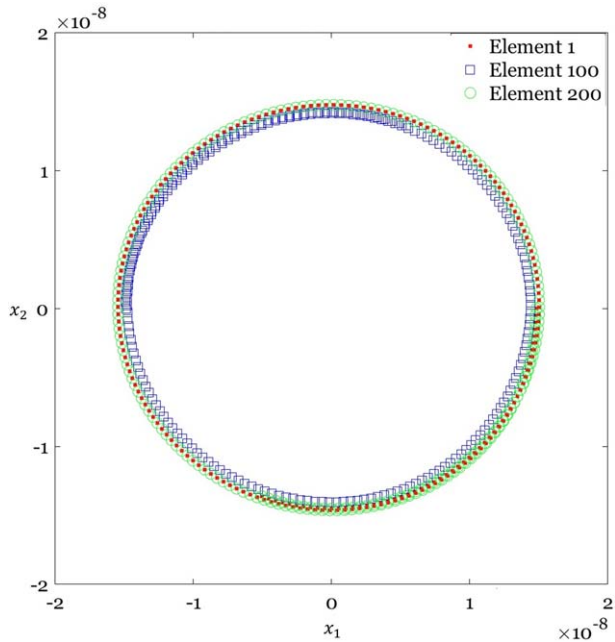


FIG. 10. (Color online) Orbits of primitives 1, 100, and 200 of the rotating cosine (relative to the primitives' geometric center).

(see Tables I and II). The question is about the convergence characteristics of a total mass composed of an increasing number of point masses that exert forces on each other that are in inverse square proportion to the square of distance. Before addressing this problem directly, note that a much simpler problem involving point masses illustrates that one can anticipate total mass decreasing as the number of point masses increases. Consider the classical, nonrelativistic analysis of a ring of N equally spaced point masses rotating about a stationary center at angular velocity ω (Fig. 11).

As the number of point masses increases, it is easy to show if the angular rate does not change that the total mass

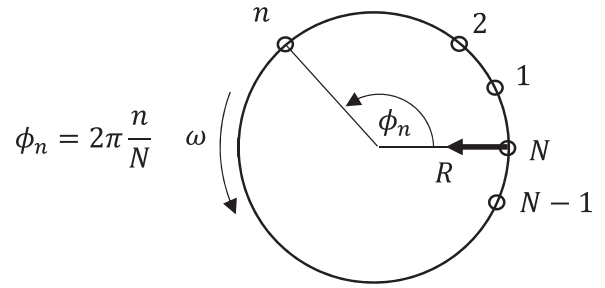


FIG. 11. Ring of N equally spaced, gravitational sources.

TABLE III. Mass per primitive versus the total number of primitives.

No. of primitives N	Mass per primitive m (kg)	Total mass M (kg)
100	5.904×10^8	5.904×10^{10}
200	2.567×10^8	5.134×10^{10}
400	1.104×10^8	4.417×10^{10}
800	4.749×10^7	3.799×10^{10}

must decrease. One calculates the force acting on point mass N and equates it to its mass multiplied by its centrifugal acceleration. One finds that the total nondimensional mass comprised of N point masses is $\bar{M}_N \triangleq (GM/4R^3\omega^2) = N \left(\sum_{n=1}^{N-1} \sin^{-1}(\phi_n/2) \right)^{-1}$. For example: $\bar{M}_{10^1} = 0.6473$, $\bar{M}_{10^3} = 0.2233$, $\bar{M}_{10^5} = 0.1350$, $\bar{M}_{10^7} = 0.0967$, $\bar{M}_{10^{11}} = 0.0617$, and $\bar{M}_{10^{12}} = 0.0566$. Convergence is decreasing but slow. With this rate in which the total mass decreases, reaching the mass of a subatomic body would require a tremendously large number of point masses.

Returning to the rotating cosine structure problem, Table III compares simulations with different numbers of primitives, showing how the mass per primitive changes with the number of primitives. We obtained the data points in the simulations by adjusting the mass per primitive to achieve a circular orbit in an $x_1 - x_2$ plane that is moving relative to the mass center in the x_3 direction.

Figure 12 shows the total mass as a function of the inverse of the number of primitives. It shows that as the number of primitives increases (as $1/N$ goes to 0). The total mass goes to zero, but at a finite value it can correspond to a photon (more about this is the discussion section). A second order power law trend line is shown. It has an R^2 value of 0.9996.

Remark: Although not shown, after sufficiently increasing the number of primitives that make up the rotating cosine function, an inherent level of roughness revealed itself. The function was not completely smooth. We anticipated this per the comments below Eq. (20). Indeed, differences in radii in Eq. (20) along the y direction cause differences in v_a , which prevent the cosine shape from staying in the x_3R plane. While a self-correcting mechanism preserves stability, small deflections perpendicular to the x_3R plane are necessary in order for the particles' speeds to stay at c , which sets up smaller scale out-of-plane behavior that limits the smoothness of the function. Indeed, one can venture that the precise shape of the rotating cosine is fractal in nature, not so

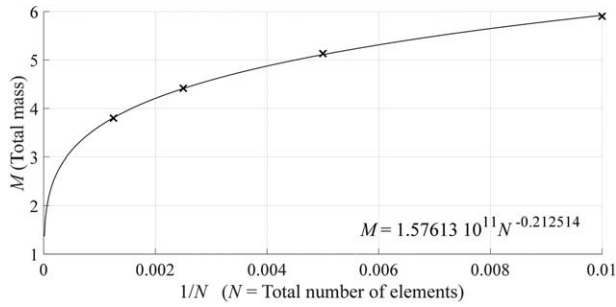


FIG. 12. Total mass M versus $1/N$.

different from the scales of physical reality that naturally divide into atoms, molecules, macro-scale bodies, celestial bodies, solar systems, galaxies, and so on.

Next, to illustrate the constrained stability methodology presented earlier, we reanalyzed the stability of the 200-primitive cosine structure, but now tested its stability by specifying the motion of a subset of its primitives. We sought to determine whether the overall structure remained stable with nominally circular orbits. Such a methodology, as mentioned, becomes particularly valuable when $n \ll N$ for extremely large N .

The first case study specified the coordinates and velocities of primitives 91–110, while we determined the motion of the remaining primitives (1–90 and 111–200) by the governing equations of motion. Figure 13 shows the orbits of primitives 1, 100, and 200. During the simulation, the geometric center of each of the three coordinates was calculated and subtracted from the coordinates. This produced a viewpoint that is relative to the structure’s centroid. This removed any net “drift,” too. We see that primitives 1 and 200 more or less track each other and remain centered on the adjusted coordinate origin, while primitive 100 (within the specified group) does drift. Having specified the motion of primitive 100 to be circular, the results were confusing. Figure 14

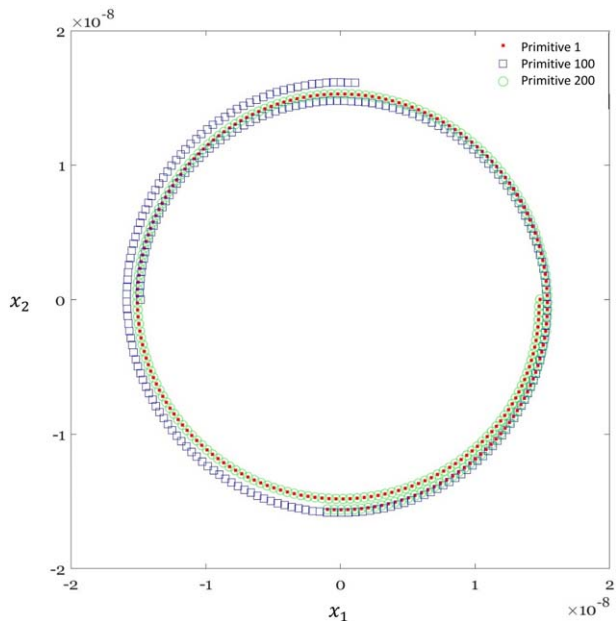


FIG. 13. (Color online) Stability test of the orbits of primitives 1, 100, and 200 of the rotating cosine (relative to the primitives’ geometric center).

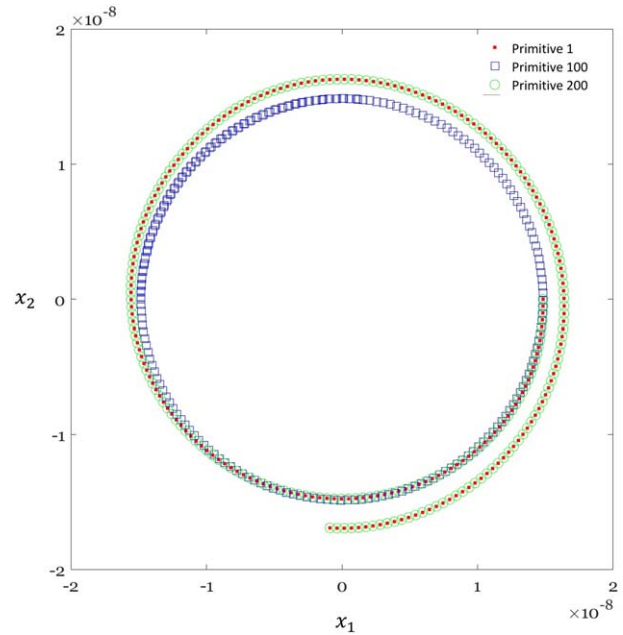


FIG. 14. (Color online) Stability test of the orbits of primitives 1, 100, and 200 of the rotating cosine (removing the subtraction of the primitives’ geometric center).

shows the result again, but this time without subtracting the average. Now primitive 100 executes the expected circular motion but primitives 1 and 200 track each other and drift.

VII. SUMMARY AND CONCLUSIONS

A historical gap in the literature motivated this study. Scientists well know that Bohr, DeBroglie, Bohm, and others dealt with atomic models that consisted of a small number of primitives. At that time, they would not have been able to model orbitals composed of a large number of primitives because of the unavailability of the computer and, as it turned out, there was no need for this, anyway. With remarkable success, the quantum-statistical approach achieved what the scientists then sought—explanations behind behaviors observed at the larger than atomic scales resulting from atomic scale considerations. However, what of the atomic structures themselves? Today, what value might quantum-deterministic descriptions offer with regard to understanding physical behavior, and do we now have the computer power to explore this?

The short answer is that in reductionism, that is, in the pursuit of understanding physical behavior through descriptions that transcend the different realms, the quantum-deterministic description might very well contribute to the state of the art. The quantum-deterministic description could fill in gaps between the quantum realm and the other realms, from the smallest (primitive) to the largest (cosmological). Furthermore, we now have strong computer tools available to assist us.

In this article, we divided the problem of the quantum-deterministic model into a kinematic problem and a kinetic problem. Given that a satisfactory quantum-deterministic model does not yet exist, the treatment required that we offer hypotheses pertaining to the corresponding kinematics and

kinetics of primitives. With regard to the kinematics, our strategy was to start with the hypothesis that the principle of light originates from distributions of bodies traveling at the speed of light, that they form the orbitals that we classically describe quantum statistically. With regard to the kinetics, our strategy was to start with the hypothesis that the principle of impetus and gravitational attraction apply to primitive bodies. As explained in the body of the article, we started with these hypotheses because they apply already in the other deterministic theories. As pointed out in the article, scientists discovered recently that the theory of general relativity conforms to the principle of impetus and gravitation in the ordinary (Minkowski) spacetime sense, which is important because scientists viewed both general relativity's kinematics and its kinetics to be an exception, which would have been an impediment to reductionism.

In addition, as mentioned, in the quantum-deterministic description, we interpreted the orbital as a distribution of a large number of bodies. Would the number be necessarily large? The answer resides in the kinematic connection between the motion of primitives and the aggregated body formed from them, and in the kinetics of a body aggregated from primitives. As described, we defined the location of an aggregated body as an average of locations of primitives. Had the number of bodies not been very large, one likely would have been able to detect the motion of an individual primitive by an emitted "primitive frequency," but that does not appear to be the case. When sufficiently large, one would then expect to observe a single "aggregated frequency," which indeed is the case. Mathematically, the Morlet wavelet ($\Psi = Ae^{-r^2/2\sigma}e^{i\omega t}$)¹⁶ is the product of the Gaussian function and the complex exponential function, in which one can think of the Gaussian function itself as a series of an immense number of functions.

Second, in this article, we showed that the ordinary (Minkowski) spacetime metric emerges from the spatial averaging of the trajectories of bodies traveling at the speed c . This also supported the idea that the number of primitives would be immense. It also supported that notion of a universal frame, in support of Newton's inertial frame and Foucault's, Mach's, and Einstein's universal frame.

The immense number of primitive bodies emerges as a potentially necessary requirement from the kinetics, too. Here, we were concerned with the number of bodies that are required to achieve a stable structure and discovered a "gravitational chain effect," apparently characteristic of the stability of bodies under the influence of a primitive inverse square law, which corresponds to the simplest form of a gravitational law that would be consistent with general relativistic behavior. The gravitational chain is a distribution. Therefore, it would appear to require an immense number of primitives. The article simulated the gravitational chain effect of an aggregated body in the shape of a rotating cosine for a comparatively small number of primitives, but we speculate that it represents a one-dimensional distribution that, in reality, has an almost countless number of primitives. Depending on the subatomic structure, the distribution could even be three-dimensional. Despite the simplicity of the model we examined, it revealed a number of properties that

one would expect to find in bodies that make up an orbital or some other subatomic structure.

To begin with, the revealed stability mechanism of the rotating cosine structure was quite different from the mechanism one finds in electrostatics and in celestial mechanics. Recall that the gravitational forces, by virtue of being perpendicular to the directions of the trajectories of the primitives, kept their speeds at c . Furthermore, the stable configurations that we found arose when the bodies were traveling in a tight formation that looked like a "flow" in the Z direction. The gravitational forces had attractive components in the Z direction and attractive components in the XY plane. The constancy of the speeds of the individual primitives in the Z direction, along with a rotation about the Z -axis, set up a stability mechanism that involved an interplay between offsets in the Z direction and motions (rotations) in the XY plane. The rotating ring example and the rotating cosine example illustrated this.

In the rotating ring example, all of the primitives were initially located in the XY plane. This example illustrated what happens when there is no initial offset in the Z direction. Although not shown in the article, the system was not in equilibrium when the bodies were not rotating. Dynamic equilibrium required a rotation of the ring primitives about an axis perpendicular to the ring. The primitives rotated about the Z -axis at just one specific rate of rotation. Furthermore, it was unstable. In the simulations, the system imploded when initially rotating slower and exploded when initially rotating more rapidly. Similar to the rotating ring example, in the spiraling two-primitive case, the circular shape in the XY plane elongated while a Z offset naturally appeared as a means of self-correcting.^{(d),(e),(f)} The stabilization of these structures of primitives required offsets in the Z direction.

In the rotating cosine example, rather than place the primitives in the XY plane at the same Z coordinate, we placed them in the shape of a cosine function along the Z -axis. When simulating the response, an interplay took place between motion in the Z direction and rotation about the Z -axis. The result was the appearance of a "gravitational chain effect."^(f)

The rotating ring structure and the rotating cosine structure illustrated that the stability mechanism is rooted in an interplay between offsets in a direction of flow together with a rotation about the axis of the direction of flow.

The rotating cosine example represents one simple structure that is stable, and there are likely many others. For instance, going back to the rotating ring problem, if in addition to rotating its primitives about the Z -axis, we could have set up the primitives so they are spiraling around the ring, too. The spiraling would then have added a component of motion along the Z direction. Early results (not presented) indicate that this stabilizes the ring, too. Other possibilities distribute the primitives over surfaces and throughout three-dimensional space. For example, there is reason to believe that one might obtain dynamic equilibrium and even stability in primitives that flow on the surface of a horn torus. We constructed an ideal horn torus structure to illustrate the flow of the primitives on its surface. As shown in a simulation of

an ideal horn torus,⁸⁾ the primitives would travel up through its center and down over the outside, or vice versa. One would then need to verify its stability by imposing initial conditions from the ideal horn torus in a simulation that imposes the inverse square law imposed on the primitives.

The prospect of stable quantum-deterministic structures leads to the follow-on question of the extent to which these structures resemble quantum-statistically described structures.

How close does the rotating cosine structure resemble a photon? The simplicity of the rotating cosine structure's string-like shape allows it to flow at speeds that are close to c but its flow cannot stop. If it were to stop, the rotating cosine structure would lose its stability. It would break apart. Furthermore, the trajectories of the rotating cosine structure that we presented were circular in the cross section perpendicular to the direction of flow. We obtained elliptical cross sections, too (not presented). Are these properties analogous to the photon? The photon, too travels at c or near c , never slows down, and has a rest mass of zero corresponding to breaking apart after slowing down. The frequency, wavelength, and energy could correspond the photon's quanta and the eccentricity of the rotating cosine structure's elliptical cross section could correspond to polarization.

Unlike for the rotating cosine structure, the geometric center of the rotating ring structure, if stabilized by spiraling motion, does not have to flow. The geometric center of the stabilized rotating ring can be stationary or move at a nonrelativistic speed. Furthermore, the rotation and spiraling together creates a left-handed and right-handed spin, and the motion of primitives whilst its center is stationary could correspond to a rest mass. How similar is the stabilized rotating ring to the electron? Could the handedness and rest state of

the stabilized rotating ring correspond to the handedness and rest states of the electron along with its mass?

Although conjectured, we based the exploration that we report on here on principles that apply to the trajectories of bodies that we took from the deterministic realms. One has to wonder whether or how well quantum-deterministic models can shed light on quantum-statistically described behavior. Could the results contained in this article provide a clue to a transcendence across physical theories that corresponds to realms that science classically sees as different?

¹A. I. Rae, *Quantum Physics: Illusion or Reality?* (Cambridge University Press, Cambridge, 2004).

²L. de Broglie, *Ann. Phys.* **10**, 22 (1925).

³D. Bohm, *Wholeness and the Implicate Order* (Routledge, London, 2005).

⁴I. Newton, *The Principia: Mathematical Principles of Natural Philosophy* (Cambridge University Press, Cambridge, 2021).

⁵J. D. Jackson, *Classical Electrodynamics* (John Wiley & Sons, Hoboken, NJ, 2021).

⁶R. Resnick, *Introduction to Special Relativity* (John Wiley & Sons, Hoboken, NJ, 1991).

⁷M. P. Hobson, G. P. Efstathiou, and A. N. Lasenby, *General Relativity: An Introduction for Physicists* (Cambridge University Press, Cambridge, 2006).

⁸L. M. Silverberg, and J. W. Eischen, *Phys. Essays* **34**, 548 (2021).

⁹H. Minkowski, *Geometrie Der Zahlen (Geometry of the Count)* (BG Teubner, Leipzig, 1910).

¹⁰E. Kreyszig, *Introductory Functional Analysis with Applications* (John Wiley & Sons, Hoboken, NJ, 1991).

¹¹H. Reichenbach, *The Philosophy of Space and Time* (Courier Corporation, North Chelmsford, MA, 2012).

¹²R. M. Wald, *General Relativity* (University of Chicago Press, Chicago, IL, 2010).

¹³D. Halliday, R. Resnick, and J. Walker, *Fundamentals of Physics* (Wiley, New York, 1997).

¹⁴L. M. Silverberg and J. W. Eischen, *J. Spacecr. Rockets* **60**, 1854 (2023).

¹⁵H. Baruh, *Analytical Dynamics* (McGraw Hill, New York, 1999).

¹⁶J. Ashmead, *Quanta* **1**, 58 (2012).

⁸⁾See <http://tinyurl.com/IdealizedHornTorusStructure> for "The horn torus."